



Comparative ecotoxicity of graphene, functionalized multi-walled CNTs, and their mixture in freshwater microalgae, *Scenedesmus obliquus*: analyzing the role of oxidative stress

Soupam Das¹ · Sayani Giri¹ · Gaurav Wadhwa¹ · Mrudula Pulimi¹ · Shalini Anand² · Natarajan Chandrasekaran¹ · Seayed Ali Johari³ · Pramod Kumar Rai² · Amitava Mukherjee¹

Received: 14 December 2022 / Accepted: 27 April 2023 / Published online: 5 May 2023
© The Author(s), under exclusive licence to Springer-Verlag GmbH Germany, part of Springer Nature 2023

Abstract

Due to their remarkable properties, the applications of carbon-based nanomaterials (CNMs) such as graphene and functionalized multi-walled carbon nanotubes (f-MWCNTs) are increasing. These CNMs can enter the freshwater environment via numerous routes, potentially exposing various organisms. The current study assesses the effects of graphene, f-MWCNTs, and their binary mixture on the freshwater algal species *Scenedesmus obliquus*. The concentration for the individual materials was kept at 1 mg L⁻¹, while graphene and f-MWCNTs were taken at 0.5 mg L⁻¹ each for the combination. Both the CNMs caused a decrease in cell viability, esterase activity, and photosynthetic efficiency in the cells. The cytotoxic effects were accompanied by increased hydroxyl and superoxide radical generation, lipid peroxidation, antioxidant enzyme activity (catalase and superoxide dismutase), and mitochondrial membrane potential. Graphene was more toxic compared to f-MWCNTs. The binary mixture of the pollutants demonstrated a synergistic enhancement of the toxic potential. Oxidative stress generation played a critical role in toxicity responses, as noted by a strong correlation between the physiological parameters and the biomarkers of oxidative stress. The outcomes from this study emphasize the significance of considering the combined effects of various CNMs as part of a thorough evaluation of ecotoxicity in freshwater organisms.

Keywords Nanotoxicology · Aquatic environment · Growth inhibition · Carbon nanomaterials · Shading effect

Introduction

Carbon-based nanomaterials (CNMs), such as graphene and functionalized multi-walled carbon nanotubes (f-MWCNTs), have great promise in developing novel materials. Graphene has excellent thermal conductivity and mechanical properties, a large specific surface area, and perfect catalytic activity. Their unique properties make them potential candidates for biomedical applications (including drug

delivery), photovoltaic devices, electrochemical devices, energy storage, and catalytic applications (Malhotra et al. 2020). Increasing production and usage of graphene lead to their uncontrolled release into aquatic systems endangering the underwater flora and fauna (Arvidsson et al. 2013; Segal 2009). f-MWCNTs find applications in various fields like electronics, nanomedicine, catalysis, and water purification (Pikula et al. 2020). Carbon-based nanoproducts are becoming more popular, with estimates predicting worldwide output could reach 10,500–20,000 tonnes by 2020 (Saxena et al. 2020). The rapid growth in the usage of CNMs leads to their release into the aquatic environments, posing a severe threat to aquatic organisms (Freixa et al. 2018; Markus et al. 2016).

Comparing the EC₅₀ toxicity data reported in the literature, algae form the most sensitive group of organisms to CNMs (Freixa et al. 2018). Current literature regarding the ecotoxicity of the CNMs centers around single species studies with the least number of reports available on algae. *Scenedesmus sp.* is a common unicellular green alga in freshwater bodies worldwide (Zhou et al. 2012). Due to its

Responsible Editor: Wei Liu

✉ Amitava Mukherjee
amit.mookerjee@gmail.com; amitav@vit.ac.in

- ¹ Centre for Nanobiotechnology, Vellore Institute of Technology, Vellore, Tamil Nadu, India
- ² Centre for Fire, Explosives and Environment Safety, Timarpur, Delhi 110054, India
- ³ Aquaculture Department, Faculty of Natural Resources, University of Kurdistan, Sanandaj, Iran

easy cultivation and intense sensitivity to aquatic pollutants, *Scenedesmus obliquus* is widely used for risk assessment. It has been used in past studies to examine the toxicity of carbon-based nanomaterials like graphene (Guo and Mei 2014) and carbon nanotubes (Stanley et al. 2016). Considering this information, *Scenedesmus sp.* was selected as a model organism to study CNM toxicity in the current work.

Though there are quite a few studies on the toxic effects of Fullerenes, MWCNTs, and SWCNTs in aquatic organisms, the toxicity of graphene needs to be better studied. There are only a handful of previous studies on graphene toxicity in aquatic organisms, even less in algae (Freixa et al. 2018). The toxicity of graphene depends on the concentration, variations within the graphene family (two-dimensional size, three-dimensional structure, and thickness), manufacturing methods, and the types of functional groups (Guo and Mei 2014). In a previous study, it was observed that exposing freshwater algae (*Chlorella pyrenoidosa*) to graphene led to a significant reduction in the membrane integrity of the cells (Zhao et al. 2014). Wang et al. (2016) also reported that graphene inhibited growth in *Scenedesmus obliquus* in a concentration-dependent manner. Guo et al. (2016) observed dose-dependent toxicity of graphene in another species, *Chlorella pyrenoidosa*. f-MWCNTs are known to impose a shading effect and inhibit algal growth (Long et al. 2012). They also generate oxidative stresses like ROS and malondialdehyde, which ultimately affects DNA in aquatic organisms (Manna et al. 2005; Thurnherr et al. 2011). Different algal species may have differences in sensitivities to CNTs. When exposed to f-MWCNTs, growth inhibition in *Chlorella vulgaris* ($EC_{50} = 1.8 \text{ mg L}^{-1}$) was quite different than that in *Pseudokirchneriella subcapitata* ($EC_{50} = 20 \text{ mg L}^{-1}$) (Schwab et al. 2011). In another study, significant growth inhibition ($EC_{50} = 17.95 \text{ mg L}^{-1}$) by CNTs was noticed in *Pseudokirchneriella subcapitata* (Lukhele et al. 2015).

Generally, a natural aquatic environment would consist of multiple types of nanomaterials. As a result, the risk and impact assessment strategy of nanomaterials in aquatic environments should consider the presence of a diverse range of co-occurring pollutants with varying cytotoxicity potentials (Bundschuh et al. 2018). Multi-walled CNTs increased the photosynthesis inhibition effect of diuron in *Chlorella vulgaris* by fivefold (Schwab et al. 2013). The mixture of MWCNTs and phenanthrene increased the immobilization of *D. magna* compared to the individual pollutants (Zindler et al. 2016). In another work, *O. niloticus* exposed to Pb^{2+} mixed with MWCNTs showed severe histopathologic alterations in the gills and decreased oxygen consumption and ammonium excretion (Barbieri et al. 2016; Martinez et al. 2013). Though there have been prior studies on the combined toxic effects of a mixture of the CNMs with inorganic and organic pollutants, the mixture effects of different CNMs are yet to be explored in algae or other aquatic organisms.

In this study, we hypothesized that f-MWCNTs and graphene exerted cytotoxicity on the algal cells by inducing oxidative stress. Their effects were further enhanced in their binary combinations. According to the best of the authors' understanding, this is the first work to analyze the combined effects of two frequently occurring CNMs, f-MWCNTs and graphene, in an equi-concentration mixture in aquatic organisms and compare the mixture effects with that of the pristine materials. The EC_{10} , EC_{50} , and EC_{90} values were determined (Table S1) for f-MWCNT and graphene in *Scenedesmus sp.* The recent literature review observed that the predicated environmental concentrations of CNT and graphene were approximately 2×10^{-5} – 1.82 ng/L (Zhao et al. 2021). Hence, a sublethal dose of 1 mg L^{-1} (less than EC_{50}) was selected for pristine CNMs in this study which was also found to be environmentally relevant according to previous studies (Zhao et al. 2021). The mixture contained 0.5 mg L^{-1} of both the CNMs keeping the total concentration at 1 mg L^{-1} . Natural freshwater (filtered and sterilized before use) was employed as the test medium to simulate the natural exposure conditions. Since both the treatment and control groups were incubated in the same lake water matrix, the natural organics and other physiochemical factors found in the lake water can be ruled out. Cell viability, superoxide and hydroxyl radical generation, membrane damage, and antioxidant enzyme activity were measured in *Scenedesmus obliquus* to determine the overall toxicity of the individual and binary mixture of graphene and f-MWCNTs. Additionally, the metabolic activity and photosynthetic efficiency were also assessed.

Materials and methods

Chemicals used

The chemicals used for this study's different experiments, including fluorescein diacetate (FDA) and Rhodamine 123 (Rh123), were purchased from Sigma Aldrich. Hydroxylamine hydrochloride, thiobarbituric acid (TBA), dimethyl sulfoxide, and trichloroacetic acid (TCA) were obtained from Hi-Media Pvt. Ltd. (Mumbai, India). Aminophenyl fluorescein (APF) and dihydroethidium (DHE) were acquired from Invitrogen™, Molecular Probes®, CA, USA. Hydrogen peroxide solution (H_2O_2 —30% w/v) and nitro blue tetrazolium chloride (NBT) were purchased from SDFCL, Mumbai, India. Functionalized multi-walled carbon nanotubes (f-MWCNT) and graphene nanoparticles used in this study were acquired from the DRDO lab (Centre for Fire, Explosives and Environment Safety, Timarpur, Delhi 110,054, India).

Isolating and sustaining the culture

For the current study, an environmentally dominant and easy-to-grow alga, *Scenedesmus obliquus*, was used for all the experiments after isolating it from the lake in VIT, Vellore (latitude—12°58'10" N, longitude—79°9'37" E). This isolated algal culture was then subcultured using the sterilized BG-11 medium purchased from Hi-Media Pvt. Ltd. This subculture was maintained in a temperature-controlled chamber (I.L.E. Co., India) at 23 ± 2 °C. A photoperiod of 16 h was maintained specifically by illuminating the cultures using a white fluorescent lamp with the illumination of 3000 lx (Philips TL-D Super 80, linear fluorescent lamp, India) to facilitate the proper growth of the cultures (Roy et al. 2018).

Lake water collection and filtration

To mimic environmental conditions, the analysis utilized freshwater as an interaction medium. For the current study, the water came from the lake at VIT University, Vellore, Tamil Nadu, India. This lake water was subjected to a series of filtration processes before being used as an interaction medium. At first, the collected lake water was passed through blotting paper thrice to remove most of the large particulate matter and debris. Following this, the collected filtrate underwent filtration through Whatman no. 1 (pore size 11 μm) filter paper to remove all possible suspended particles. Finally, after the filtrations, the collected filtrate was sterilized in an autoclave at 121 °C for 15 min. This collected lake water followed a series of filtrations, and sterilization was referred to as the freshwater medium in the study and was henceforth used for all the interaction experiments (Roy et al. 2020). Table S2 represents the physiochemical characteristics of lake water before and after filtration and sterilization. Natural organics and other physiochemical factors in lake water cannot affect the treatment or control groups since both were incubated in the same lake water matrix.

Stock solution preparation of CNMs

For the current study, the stock solutions were prepared in deionized water. The individual nanoparticles (NPs), namely, graphene and f-MWCNTs, were dispersed in lake water at the concentration of 1 mg L^{-1} . To secure the proper dispersion of the particles, the suspensions were ultrasonicated for 30 min (130 W, 20 kHz; Sonics, USA). To prepare the binary mixtures, 0.5 mg L^{-1} of graphene and 0.5 mg L^{-1} of f-MWCNT were mixed and ultrasonicated. The intended working concentration for the mixture was held constant at 1 mg L^{-1} .

Physicochemical characterization

To determine the surface characteristics of the nanoparticles, the suspensions of graphene and f-MWCNT were subjected to a super-resolution field emission scanning electron microscope (FE-SEM). The sample suspensions were coated on a glass slide and sputter coated with gold for proper viewing under the scanning electron microscopes Thermo Fisher FEI Quanta 250 FEG for f-MWCNT and Carl Zeiss EVO/18 Research for graphene. To determine the aggregation pattern of the nanoparticles after 72 h, the suspensions of graphene and f-MWCNT were subjected to FE-SEM analysis (Thermo Fisher FEI Quanta 250 FEG). An X-ray diffractometer was used to confirm the crystallinity of the NPs (Advanced D8, Bruker, Germany). Fourier-transform infrared spectroscopy (FTIR) was done for the graphene and f-MWCNT samples to confirm the significant functional groups present in the samples.

The sedimentation study of f-MWCNT, graphene, and their binary mixture was performed to monitor the colloidal stability of the nanoparticles in the lake water medium. After dispersing the nanoparticles in the medium, the solution was held on a stable platform for 72 h. The samples were collected every few hours from the top layer of the solution. The absorbance of the collected samples was determined using a UV–Vis spectrophotometer at 260 nm and 270 nm for f-MWCNT and graphene, respectively.

Algal interactions with NPs

For the interaction studies, late log phase algal culture was centrifuged and set at the optical density of 0.5. After setting the optical density of the algal cells at the optimum, these cells were kept for a 72-h interaction with the nanoparticles. For individual interactions, the concentration of graphene and f-MWCNT was maintained at 1 mg L^{-1} , and for the binary mixture, both the nanoparticles (f-MWCNT and graphene) were kept at 0.5 mg L^{-1} . Finally, the total volume was made up to 5 mL by adding filtered, sterilized lake water. These interactions were carried out under visible light conditions at 23 °C for 72 h (Roy et al. 2021). The OECD guidelines (2004) were strictly followed during toxicity testing. The algal sample was kept for the experiments in each combination with an appropriate control that did not include the contaminant mixtures. They were all performed in triplicates to get statistically significant results from any of the experiments ($n = 3$) (OECD 2004).

The effect of light shading by nanoparticles on algal growth suppression and photosynthetic efficiency was examined following a previous study (Zhao et al. 2017). Figure S6 depicts the experimental setup of the shading effect. Briefly, 100-mL conical flasks containing exponentially developing algal cells were put in 500-mL beakers containing

nanoparticle suspensions (1 mg L^{-1}) previously prepared in the lake water medium. The nanoparticle suspension level in the beaker was maintained at the same level as the algal suspension level in the conical flask. After 96 h of shading in nanoparticle suspension, the number of algal cells in conical flasks was determined. Treatment with the lake water medium without the nanoparticles was taken as a control.

Cell viability evaluation

The cell numbers (without morphological damage) were obtained after 72 h of exposure by loading $10 \mu\text{L}$ of algal cell suspension for all the control and treated samples into a Neubauer counting chamber placed under an optical microscope (Zeiss Axiostar Microscope, USA). At last, the percentage of viable cells for samples treated with graphene, f-MWCNT, and their binary mixture was calculated with respect to control using the formula below (Thiagarajan et al. 2019).

$$\% \text{ Cell viability} = \frac{(\text{No. of cells in control sample} - \text{No. of cells in test sample})}{\text{No. of cells in control sample}} \times 100$$

Analyzing oxidative stress

Superoxide radical generation

Dihydroethidium (DHE), a fluorescence dye, was utilized to detect the superoxide radical produced by algal cells. The blue fluorescent dye dihydroethidium (DHE) detects superoxide radicals produced within algal cells by reacting with the radicals and converting them to red fluorescent ethidium (Owusu-Ansah et al. 2008). Our previous investigations describe the procedure fully (Natarajan et al. 2020). Interacted algal samples were incubated in the dark with DHE dye (10 mM) for 30 min. Following incubation, a fluorescent spectrophotometer was employed to measure the fluorescence intensity of the interacted algal samples at excitation and emission spectra of 480 and 570 nm, respectively (Cary Eclipse fluorescence spectrophotometer, model G9800A; Agilent Technologies, USA).

Hydroxyl radical generation

Aminophenyl fluorescein (APF) is a dye that was used to measure the generation of hydroxyl radicals by reacting with high reactive oxygen species (hROS), specifically the hydroxyl radical ($\bullet\text{OH}$) (Setsukinai et al. 2003). The experimental approach used to calculate OH \cdot radical generation was based on previous studies (Natarajan et al. 2020). The APF dye interacted with the treated algal pellets and was kept for 30 min of dark incubation. The fluorescence

intensity of the incubated algal samples was measured at excitation and emission spectra of 490 and 515 nm, respectively.

Lipid peroxidation and antioxidant enzyme assay

The damage to algal cell membranes caused by lipid peroxidation induced by the nanoparticles was estimated indirectly by measuring malonaldehyde (MDA) production. The algal cultures, after the interaction, were centrifuged at $4 \text{ }^\circ\text{C}$ for 10 min at 7000 rpm. The obtained cell pellet was treated with 0.25% TBA (prepared in a 10% TCA solution) and heated in a water bath at $95 \text{ }^\circ\text{C}$ for 30 min. The heated sample mixtures were quickly placed on ice to stop the reaction. The sample mixture was centrifuged at 7000 rpm for 10 min, and the supernatant's absorbance containing the released MDA enzyme was measured at 530 nm. By subtracting the absorbance at 600 nm, the nonspecific turbidity was rectified (Piotrowska-Niczyporuk et al. 2012).

The comprehensive method for analyzing superoxide dismutase (SOD) activity may be found in Kono (1978). After incubation, the algal cells were collected by centrifugation at 7000 rpm for 10 min at $4 \text{ }^\circ\text{C}$; they were then washed, homogenized in 0.5 M phosphate buffer, and subjected to the second round of centrifugation at 13,000 rpm for 20 min at $4 \text{ }^\circ\text{C}$. After the supernatant had been collected, it was then mixed with a variety of other chemicals. These contained hydroxylamine hydrochlorides at a concentration of 20 mM, nitro blue tetrazolium chloride at a concentration of 96 mM, Na_2CO_3 buffer at a concentration of 50 mM with a pH of 10, and Triton X-100 at a concentration of 0.6 percent. After being illuminated with light for a time span of 20 min, the reaction mixture was analyzed using a UV–Vis spectrophotometer reader (xMARK microplate absorbance spectrophotometer, BIO-RAD) at a wavelength of 560 nm.

The catalase (CAT) activity was measured using a modified protocol described previously (Chakraborty et al. 2021). Following treatment for 72 h, the algal cells were centrifuged at a temperature of $4 \text{ }^\circ\text{C}$ for 10 min at 7000 rpm. The cells were washed and homogenized with sterile 0.5 M PBS before being centrifuged again to isolate the supernatant. Using a spectrophotometer (Hitachi U-2910 Japan), the absorbance decrease was recorded at 240 nm for 3 min after adding 1 mL of freshly made H_2O_2 solution (10 mM) to 2 mL of supernatant. The reaction solution lacking H_2O_2 was treated as a blank.

Esterase activity and mitochondrial membrane potential (MMP)

Esterase activity and mitochondrial membrane potential were measured to evaluate the metabolic activity of the algal cells. The procedure used fluorescein diacetate (FDA) to quantify the esterase activity produced inside the algal cells for all the control and treated samples. A stock suspension of the fluorescent dye, FDA (169 mM), was prepared in acetone and stored at $-20\text{ }^{\circ}\text{C}$. For 7 min at room temperature, 400 μL of the algal sample was incubated with 300 μL of FDA (0.96 mM) solution. The fluorescent intensity of the treated samples was measured using a fluorescence spectrophotometer after incubation at excitation and emission wavelengths of 485 and 530 nm, respectively (Rudi et al. 2002).

The fluorescent dye Rhodamine 123 was used to measure the mitochondrial membrane potential (MMP). After the interaction, the algal cell pellet was separated using centrifugation (2500 g for 5 min), suspended in a 0.1 mol L^{-1} PBS buffer, and stained using a 2.5 mmol L^{-1} dye solution in the dark at $25\text{ }^{\circ}\text{C}$ for 30 min. Following the staining process, the cells were washed before being suspended in PBS. A fluorescence spectrophotometer was then used to measure the fluorescence intensity at excitation and emission wavelengths of 485 nm and 530 nm, respectively. As a reference, the data was plotted using untreated control samples (Machado and Soares 2015).

Determination of photosynthetic yield

To determine the toxicant's stress on algal photosystem II, a photosynthetic yield analyzer was used to detect chlorophyll fluorescence as well as the electron transport rate (ETR) in the treated algal samples (PS II) (Mini PAM, Heinz Walz, Germany). The samples were kept in the dark for 30 min before being analyzed. 200 μL of the interacted algal samples was loaded into the Photosynthesis Yield Analyzer (Mini PAM) chamber, and the Fv/Fm ratio and the ETR max

value were measured using a high-intensity actinic light. Variable fluorescence is Fv, while maximum fluorescence is Fm. The results were represented graphically with respect to control samples (Romanowska-Duda et al. 2019).

Statistical analysis

All experiments in the study were run in triplicate ($n=3$) to demonstrate statistical significance. Each experiment was repeated at least twice to ensure reproducibility. The data are all presented as mean \pm SD (standard deviation). A two-way ANOVA test with a Bonferroni post-test was used in GraphPad Prism 6 to test statistical significance for different test samples versus controls. Data with $p < 0.05$ was considered statistically significant ($p < 0.05$ denoted significance at the 95% confidence level).

Abbott's statistical model assessed nanoparticle interactions in the binary mixture, such as synergism, antagonism, or addition. Abbott's modeling is extensively utilized to evaluate the effect of toxicants in the context of a natural mortality cause. In the case of binary mixes, it is also the best technique to compare observed inhibitions with expected growth inhibitions (Iswarya et al. 2015).

Results

Characterization of the carbon nanomaterials

The morphology and the size of the f-MWCNT and graphene particles were analyzed using the FE-SEM images given in Fig. 1. From the images, the f-MWCNT particles were long and fibrillar, whereas the graphene particles were amorphous, forming a multi-layered sheet structure. The width of the f-MWCNT particles was around $\sim 34\text{ nm}$, but the multi-layered structure of graphene made it challenging to estimate the exact size of the graphene particles. Agglomeration between the nanoparticles was observed when dispersed in Milli-Q water (Fig. S1).

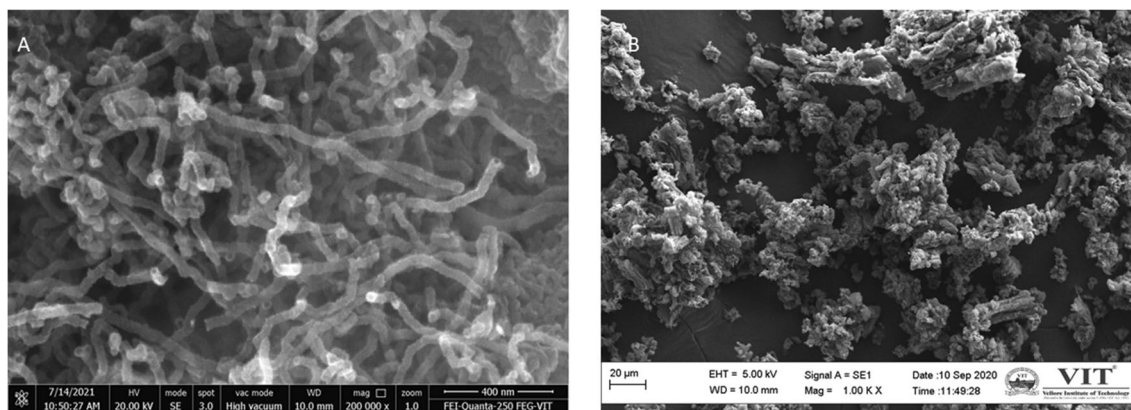


Fig. 1 FE-SEM images of **A** functionalized multi-walled CNTs (f-MWCNTs) and **B** graphene nanoparticles in the filtered lake water medium

The aggregation of nanoparticles was analyzed using FE-SEM images shown in Fig. S2. From the images, pristine f-MWCNT particles aggregated after 72 h of incubation (Fig. S2A). Similarly, pristine graphene also showed aggregation after 72 h (Fig. S2B). The binary mixture formed heteroaggregation between f-MWCNT and graphene. A heteroaggregation between f-MWCNT and graphene was also observed when mixed together (Fig. S2C).

The XRD spectra (Fig. S3A) of the f-MWCNTs showed a broad diffraction peak at $2\theta = 25.5^\circ$ corresponding to the (002) plane of graphite carbon atoms and $2\theta = 43.5^\circ$ matched to the (100) planes of the MWCNTs. The FTIR spectra (Fig. S3B) showed four bands: a band at 3418 cm^{-1} corresponding to O–H stretching mode, a band at 2980 cm^{-1} for C–H stretch, a band at 1550 cm^{-1} corresponding to C=C stretching mode, and 950 cm^{-1} for C–C–C bending mode of the inherent MWCNT structure (Li et al. 2003). The XRD for graphene particles (Fig. S4A) shows peak observed (120) can be attributed to graphene at $2\theta = 22.52^\circ$, confirming the compound to be graphene. Figure S4B represents the FTIR spectra of graphene nanoparticles. The peaks at 1040 cm^{-1} and 1160 cm^{-1} correspond to the vibrational mode of the C–O group. The peak at 1530 cm^{-1} arises from the vibration mode of the amide linkage group (CO–NH). The peak observed at 1730 cm^{-1} was assigned to the carboxyl group (C=O). The peak at 3026 cm^{-1} was attributed to the presence of the C–H bond. Peaks at 3417 cm^{-1} in the high-frequency area are attributed to the stretching mode of the O–H bond, which reveals the presence of hydroxyl groups (Saravanan et al. 2014). Absorption spectra for both f-MWCNT and graphene were shown to decrease with time in the sedimentation study (Fig. S5). The sedimentation point was found to be achieved at the end of 24 h for f-MWCNT, but for graphene, it took somewhat longer than 24 h. The sedimentation point of f-MWCNT in a binary mixture was achieved after 12 h, whereas that of graphene was reached after 16 h.

Cell viability assessment

The impact of graphene and f-MWCNT nanoparticles on the algal cells was determined by evaluating their cell viability. Figure 2 gives a graphical representation of the cell viability assessment compared to the control group. Notably, f-MWCNTs showed minimal toxicity, decreasing viability by $\sim 6\%$. Conversely, graphene showed comparatively higher toxicity, reducing cell viability by $\sim 15\%$. The toxic potential was enhanced in the binary mixture. In this case, the drop in cell viability was $\sim 25\%$.

The algal growth was significantly reduced by the shading effect of f-MWCNT, graphene, and graphene + f-MWCNTs (Fig. S7). Pristine f-MWCNT and pristine graphene

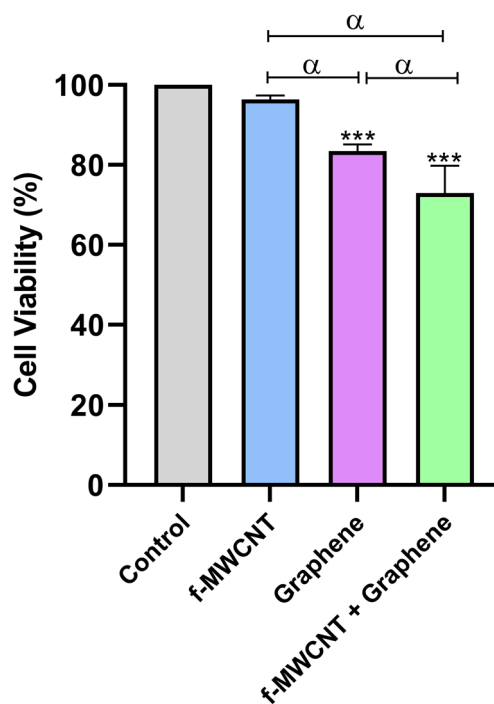


Fig. 2 The comparison of cell viability of *Scenedesmus obliquus* cells exposed to individual and binary mixtures of f-MWCNT and graphene nanoparticles. The level of significance with respect to control was represented by “***” and “α” ($p < 0.001$)

shading caused 0.56% and 4.03% of the total growth inhibition, respectively. The binary mixture caused 1.88% of the total growth inhibition, as calculated from the algal growth results. The contribution of the shading effect to the total toxicity was then calculated as 15.57% for f-MWCNT, 24.39% for graphene, and 6.96% for a graphene-f-MWCNT mixture.

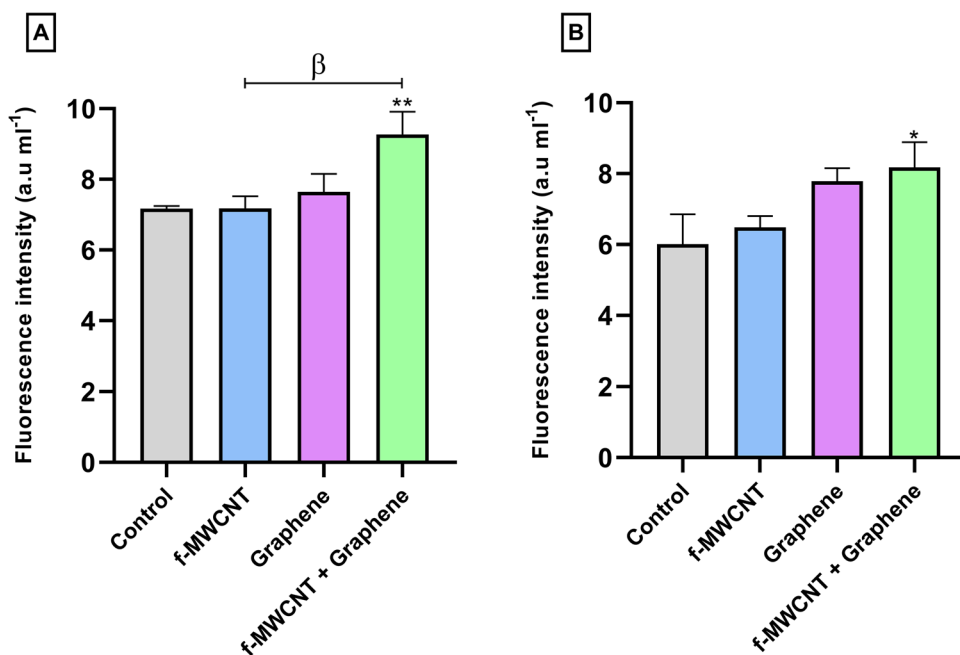
Abbott’s modeling used the growth inhibition results to determine the type of nanoparticle interactions in the binary mixture. The results found that the ratio of inhibition (RI) was 1.376, which is > 1 . Hence, we can conclude that the interactions in the binary mixture of graphene and MWCNT were synergistic.

Oxidative stress analysis

The effect of graphene and f-MWCNT on superoxide and hydroxyl radical generation in the treated cells is shown in Fig. 3A, B. Both f-MWCNT and graphene had no impact on the production of superoxide radicals compared to the control. However, the binary mixture of graphene and f-MWCNTs showed a significant increase in the radical generation by approximately ~ 1.3 times compared to the control.

Hydroxyl radical generation, on the other hand, showed a different trend. The increase in hydroxyl radical followed this order—f-MWCNT < graphene < binary mixture of

Fig. 3 Oxidative stress caused by individual and binary mixture exposure to f-MWCNT and graphene nanoparticles (presented in RFU, relative fluorescent units). **A** Superoxide radical production. **B** Hydroxyl radical production. The level of significance with respect to control was represented by “***” ($p < 0.01$), “**” and “ γ ” ($p < 0.05$). The data are the averages of at least three independent experiments ($n \geq 3$); the standard deviations are shown (vertical error bars). The mean values were represented using a two-way ANOVA test with a Bonferroni post-test



graphene and f-MWCNT. The radical generation increase compared to control was approximately ~ 1.08 times for f-MWCNT treatment, ~ 1.3 times for graphene, and finally ~ 1.36 times for binary mixture.

Lipid peroxidation and antioxidant enzyme activity

The amount of malonaldehyde (MDA) generated on treatment with the CNMs is graphically represented in Fig. 4. This MDA generation was correlated significantly to oxidative stress generation. It can be considered a direct measure of membrane damage. The lowest MDA production compared to the control was observed in the f-MWCNT-treated algal cells, approximately ~ 1.34 times the control value. It was followed by the graphene-treated cells, which were almost ~ 1.61 times higher than the control. Lastly, the most increased MDA generation was observed in the binary mixture of f-MWCNT and graphene, which showed ~ 2.18 times increment compared to the control.

The SOD and catalase activity in the CNM-treated cells is graphically represented in Fig. 5A, B. SOD activity results followed a similar trend as the oxidative radical generation and MDA production results. The increase in the SOD activity of the various CNM-treated samples followed the order f-MWCNT < graphene < binary mixture. f-MWCNTs showed an increment in SOD activity by almost ~ 1.25 times compared to the control, followed by graphene, which showed a rise in activity by ~ 1.32 times. Finally, the binary mixture showed the maximum increase in SOD activity (~ 1.5 times in comparison with the control).

Catalase activity results also showed a similar trend as the SOD activity. The lowest catalase activity was found in f-MWCNT-treated samples, which were approximate ~ 1.13 times higher than the control. This was followed by graphene particles, which were ~ 1.37 times more than the control values. The binary mixture of f-MWCNT and graphene significantly showed the maximum catalase activity, which was ~ 1.84 times higher than the control samples.

Metabolic activity analysis

The metabolic activity in the algal cells determined by mitochondrial membrane potential and esterase activity is shown in Fig. 6A, B. The mitochondrial membrane potential increased compared to the control after treatment with CNMs. The increase was the highest in the binary mixture of graphene and f-MWCNT. The mixture showed a significant rise in ~ 3.95 times compared to the control. Whereas samples treated with f-MWCNT showed the lowest mitochondrial membrane potential, almost ~ 1.37 times with respect to the control.

The esterase activity significantly decreased the treated samples compared to the control. The activity was the highest for the samples treated with f-MWCNT nanoparticles, which were ~ 0.66 times lower compared to control samples. This was followed by graphene nanoparticles whose activity was ~ 0.63 times lower than control samples. The lowest activity was found in the samples treated with the binary mixture of graphene and f-MWCNTs, which was ~ 0.57 times lower in comparison to the control samples.

Photosynthetic activity

The effects of the CNMs on the maximum quantum yield of PS II (Φ_m) and the electron transport rate in the algal cells are represented in Fig. 7A, B. There was an overall decrease in both Φ_m and electron transport rate for all the treated samples compared to the control samples. Among them, the f-MWCNT-treated samples had the highest Φ_m and electron transport rates, which were ~ 0.78 times and ~ 0.91 times lower than the control samples. Consecutively, graphene and binary mixture treated samples showed a similar decline in both Φ_m and electron transport rates, which were ~ 0.8 times and ~ 0.7 times lesser than the control samples.

The PS II activity and electron transport rate were significantly reduced by the shading effect of f-MWCNT, graphene, and graphene + f-MWCNTs (Fig. S8). The contribution of the shading effect to the total PS II inhibition was observed to be 8.46% for f-MWCNT, 16.87% for graphene, and 11.98% for a graphene-f-MWCNT mixture. Similarly, the contribution of the shading effect to the electron transport rate inhibition was observed to be 19.47% for f-MWCNT, 28.99% for graphene, and 23.24% for the binary mixture.

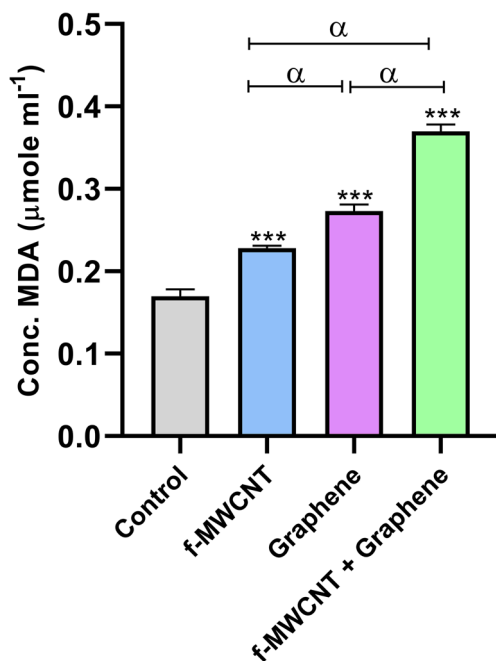


Fig. 4 Impact of the individual and binary exposure to f-MWCNT and graphene nanoparticles on the MDA content of *Scenedesmus obliquus*. The level of significance with respect to control was represented by “***” and “ α ” ($p < 0.001$). The data are the averages of at least three independent experiments ($n \geq 3$); the standard deviations are shown (vertical error bars). The mean values were represented using a two-way ANOVA test with a Bonferroni post-test

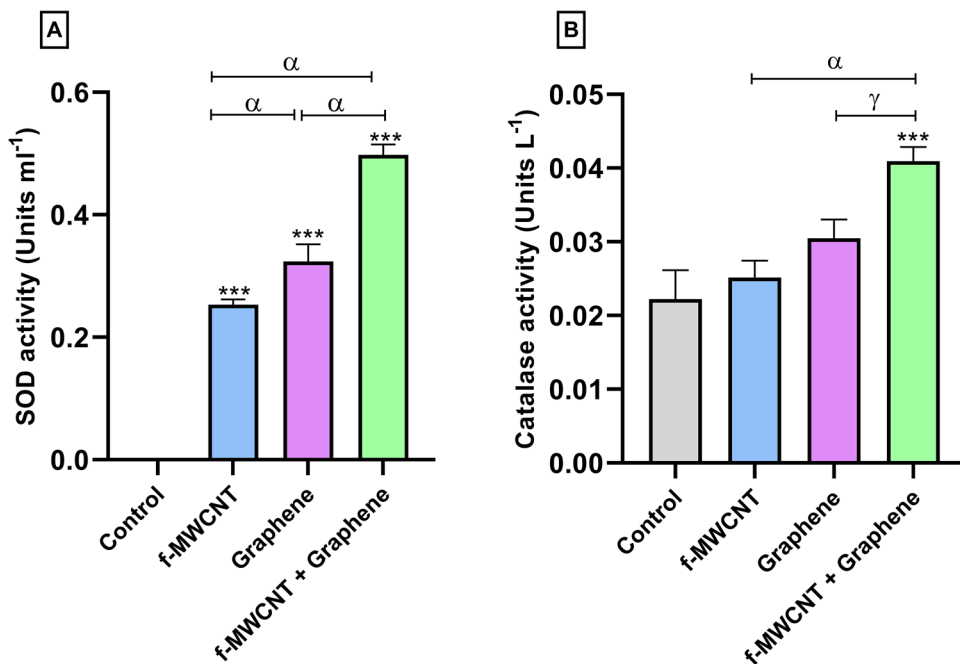
Discussion

Graphene caused higher growth inhibition than f-MWCNT in *Scenedesmus obliquus*. In previous work, Zhao et al. (2017) observed graphene as more toxic than CNTs. FE-SEM images revealed aggregation of the nanoparticles after 72 h of incubation. After 24 h, nanoparticles aggregated similarly, as sedimentation experiments showed. Agglomerates are formed due to the high attachment ability between nanoparticles, which is caused by the Brownian motion of the nanoparticles as they move through the lake water medium (Christian et al. 2008). These aggregated nanoparticles may sink to the bottom of the beakers due to the effects of gravity and might form heteroaggregates with algae, thereby increasing toxicity (Lv et al. 2016). Previous researchers also observed single-walled carbon nanotube sediment at the bottom of the vessel, increasing the toxicity to microalgae and other aquatic organisms (Parks 2013). As stated in the literature, the nanomaterials’ sedimentation was likely accelerated because sediment in the system can affect the ionic strength of the surrounding water phase. The presence of natural organic matter (NOM) in the water bodies also helps to modify the nanomaterials’ sedimentation rate (Politowski et al. 2021). It was observed in the present study that the presence of considerable amount of NOM in the water medium leads to the aggregation of particles within the medium, thereby causing them to sediment out of the medium.

Several previous studies on CNM toxicity highlighted the role of shading effects. The dispersed NPs in the medium can lessen light availability to the algal cells (Long et al. 2012). Thus, indirect toxicity through the shading effect of the CNMs was studied in this work (Fig. S4, S5). Though graphene caused a minimal decrease in algal growth through shading effects, f-MWCNT and the mixture showed almost negligible impact. Graphene’s hydrophilic surface and high electrostatic repulsion between the individual graphene sheets might explain its shading effect (Zhao et al. 2017). Although f-MWCNT was less potent than graphene, it caused growth suppression. This may be attributed to nutrient depletion and heteroaggregation with the algal cells (Kwok et al. 2010; Wei et al. 2010). The toxicity of MWCNT in algae has also been mentioned in several previous studies (Long et al. 2012; Schwab et al. 2011).

The mixture of f-MWCNT and graphene induced higher toxic effects than the individual constituents. The enhanced toxic effects of the mixture might be related to the internalization of f-MWCNT through the already damaged cell membranes by graphene (Roy et al. 2021). Since both nanomaterials used in the study are from the same family, i.e., carbon materials, they were expected to show the same mode of action, i.e., synergistic, to induce toxicity in algal

Fig. 5 Antioxidant enzyme activity in *Scenedesmus obliquus* exposed to individual and binary mixtures of f-MWCNT and graphene nanoparticles. **A** SOD activity. **B** Catalase activity. The level of significance with respect to control was represented by “***” and “ α ” ($p < 0.001$), “ γ ” ($p < 0.05$). The data are the averages of at least three independent experiments ($n \geq 3$); the standard deviations are shown (vertical error bars). The mean values were represented using a two-way ANOVA test with a Bonferroni post-test



cells. Hence, Abbot’s modeling determined their interactions in a binary mixture. Even though it was thought that the effects of CNTs were caused by the clustering of cells around nanoparticles, this was often not the case (Schwab et al. 2011). Increased heteroagglomeration of the algal cells with the CNMs in the mixture could be another reason for decreased cell viability (Freixa et al. 2018; Guo et al. 2011). The agglomerated CNMs could get adsorbed onto the algal cells, impeding the movement of nutrients and electrolytes

across the cell membrane (Lin 2008). One of the key factors that contributed to the toxicity of the binary combination was the interfacial interactions between the components of the algal cell wall and the CNMs. This can potentially damage the cell wall and promote the internalization of the nanoparticles (Zhang et al. 2015). It was observed that heteroagglomeration with other NPs (such as CNTs and Ag NPs) led to algal cell growth inhibition (Zhang et al. 2016). A recent study showed that MWCNT and CuO nanoparticles

Fig. 6 Metabolic enzyme activity in *Scenedesmus obliquus* exposed to individual and binary mixtures of f-MWCNT and graphene nanoparticles. **A** Mitochondrial membrane potential. **B** Esterase activity. The level of significance with respect to control was represented by “***” and “ α ” ($p < 0.001$). The data are the averages of at least three independent experiments ($n \geq 3$); the standard deviations are shown (vertical error bars). The mean values were represented using a two-way ANOVA test with a Bonferroni post-test

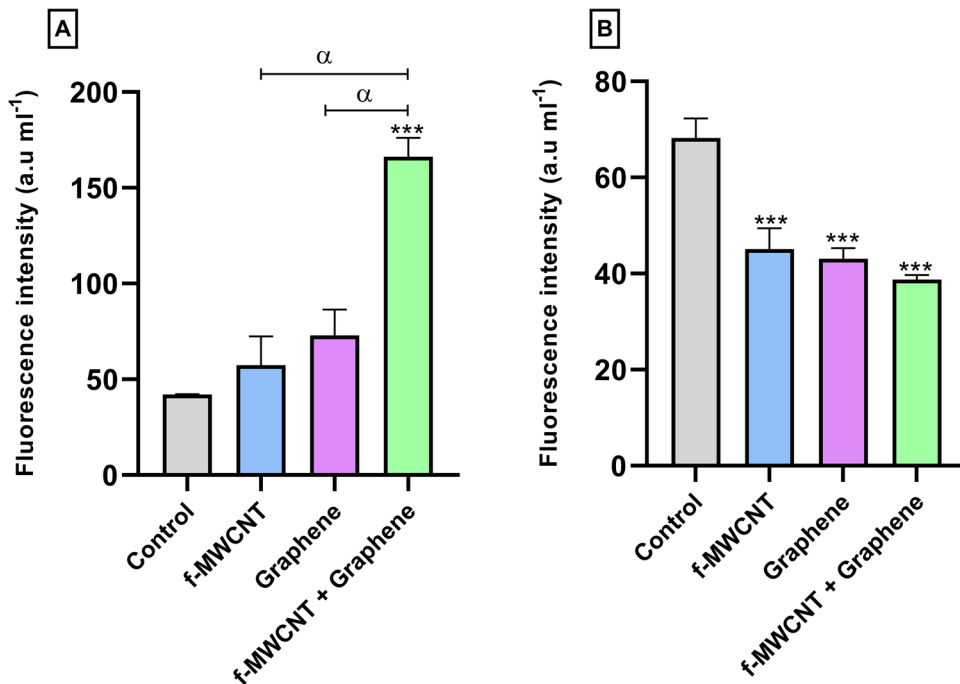
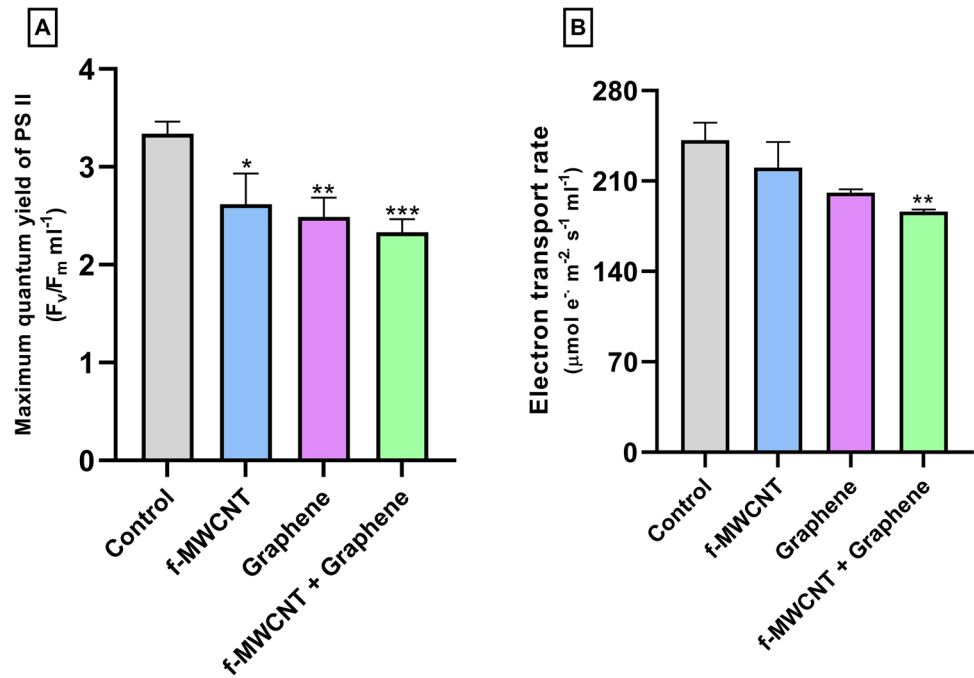


Fig. 7 Photosynthetic parameters in *Scenedesmus obliquus* exposed to individual and binary mixtures of f-MWCNT and graphene nanoparticles. **A** Maximum quantum yield of PS II (Φ_m). **B** Electron transport rate. The level of significance with respect to control was represented by “****” ($p < 0.001$), “***” ($p < 0.01$), and “**” ($p < 0.05$). The data are the averages of at least three independent experiments ($n \geq 3$); the standard deviations are shown (vertical error bars). The mean values were represented using a two-way ANOVA test with a Bonferroni post-test



combined caused growth inhibition and cell membrane damage to *Tetrademus obliquus* by getting adsorbed onto the cell surface (Fang et al. 2022).

Photosynthetic organisms constantly generate free radicals as by-products of several metabolic processes in mitochondria, chloroplasts, and peroxisomes (Hu et al. 2023). The production of oxidative radicals is exacerbated by various environmental stressors such as infections, drought, intense light, and pollutants (Liu et al. 2007; Rezayian et al. 2019). When the algal cells were treated with pristine and combined CNMs, an increase in free radical (superoxide and hydroxyl) production was noted. These effects were more predominant in the graphene-treated samples compared to the f-MWCNT-treated samples. Graphene can function as an electron suppressor, producing excess superoxide and hydroxyl radicals (Begum & Fugetsu 2013). Intracellular ROS production in graphene-treated cells can also be attributed to its sp^2 hybridized electron structure, which can directly accelerate the electron transfer between the edges of graphene and bio-membranes (Zhao et al. 2014). The shading effect might also contribute to the generation of oxidative stress. The nanoparticles prevent light from reaching the algal cells; thus, the photosynthetic activity gets disrupted, leading to increased oxidative stress (Vargas-Estrada et al. 2020; Wang et al. 2023). Long et al. (2012) observed a decrease in cell viability and increased oxidative stress of *Chlorella* sp. due to the shading effects of MWCNT, which corroborates our findings. Similarly, another study found that the primary toxic mechanism of graphene oxide to algae *Scenedesmus obliquus* was due to oxidative stress caused by the shading effects (Yin et al. 2020b).

The reactive oxygen species may cause damage to the cell membrane by reacting with polyunsaturated fatty acids (Borza et al. 2013). Oxidative radical generation leads to lipid peroxidation (Kim et al. 2022). Lipid peroxidation results in the formation of pores and increased membrane damage (Van der Paal et al. 2016). Higher cytotoxicity by graphene than the f-MWNTs can be related to the enhanced cell membrane damage caused by graphene. Yin et al. (2020a) also observed graphene-induced cell membrane damage in *Scenedesmus obliquus*. An investigation using molecular dynamics demonstrated that a graphene sheet could destructively extract lipid molecules from a double membrane layer by either (1) directly penetrating the membrane when the appropriate geometric orientation is present or (2) lying flat on the surface of the bilayer and producing a patch of upturned phospholipids (Dallavalle et al. 2015). Like our study, Yin et al. (2020b) observed increased MDA content in freshwater algae *S. obliquus* when treated with graphene oxide. The present work enhanced LPO production when the algal cells were treated with the binary mixture of graphene and f-MWCNT. A previous study on the effects of f-MWCNT combined with copper oxide in freshwater algae *Tetrademus obliquus* also reported increased lipid peroxidation (Fang et al. 2022). Oxidative stress generation is considered one of the significant contributors to direct algal toxicity of CNTs (Hu et al. 2015b; Zhu et al. 2016).

To keep ROS and radical generation at a reasonably steady level and to protect organisms from oxidative stress, antioxidant enzymes (such as SOD and CAT) could selectively catalyze the transformation of $O_2\bullet$ and H_2O_2 into oxygen and water. As a result, the antioxidant enzymes are

considered the most sensitive indicators for various environmental stressors (Hu et al. 2015a; Liu et al. 2022). With an increase in oxidative stress, the activity of the antioxidant enzymes would also increase (Finaud et al. 2006). Increased activities of SOD and CAT reveal an improved capacity of *S. obliquus* to scavenge the $O_2\bullet$ and H_2O_2 radicals generated in response to graphene and the binary mixtures (Zhang et al. 2019). A recent study by Zhu et al. (2022) observed increased SOD activity in microalgae *Gymnodinium* treated with graphene quantum dots and graphene quantum dots-ZnO mixtures. Similarly, increased CAT activity was observed by Zhang et al. (2019) when *Scenedesmus obliquus* was treated with graphene oxide for 72 h. In another work, after treating *Chlorella vulgaris* with silver-reduced graphene oxide (Ag-rGO) mixture, an increase in SOD and CAT activities was noticed (Nazari et al. 2020).

The photosynthetic activity decreases with the increase in oxidative stress for graphene, f-MWCNT, and the binary mixture. The electron transport rate also declines with the increase in oxidative stress, following the same trend as photosynthetic activity (Wang et al. 2020). Damage to the cell membrane and the subsequent internalization of the graphene nanoparticles may explain why graphene affected the photosynthetic activity of the cells more severely than f-MWCTs. Decreased cell viability and reduced photosynthetic activity were observed in marine alga *Picochlorum sp.* due to the internalization of graphene oxide (Hazeem et al. 2017). f-MWCNT-interacted algal samples also showed a minor decrease in photosynthetic activity. This might be due to indirect toxicity like light shading effects (Freixa et al. 2018). In the current study, the treatments with the binary mixture significantly lowered photosynthetic activity and electron transport rate in the algae. Presumably, the CNMs in the mixture may adsorb on the surface of the algal cells and prevent light from reaching photosynthetic centers. This would harm the electron transport rate and photosynthetic activity (Li et al. 2023). According to Sousa et al. (2018), NiO nanoparticles adsorbed on the surface of the algal cells (*Pseudokirchneriella subcapitata*) caused a reduction in the flow rate of electrons through the photosynthetic chain. Similar to our study, Cruces et al. (2021) also observed a decline in the photosynthetic activity of *Microcystis aeruginosa*, when treated with the combination of graphene oxide and oxidized multi-walled carbon nanotubes. The shading effect also affected the electron transport chain, which affected the photosynthetic centers and decreased photosynthetic activity. According to Hu et al. (2015a), the shading effect generated by graphene oxide resulted in the growth suppression of *Euglena gracilis* via a reduction in its photosynthesis. Similar to our study, Nogueira et al. (2015) observed a decrease in cell viability of *Raphidocelis subcapitata* due to light blockage and, in turn, affected the photosynthetic centers by shading effects caused by graphene oxide.

It has been hypothesized that nanoparticle exposure promotes ROS production by disrupting the mitochondrial electron transport chain. The MMP of the algal cells treated with graphene alone and binary mixes of graphene and f-MWCNT showed a noticeable increase. A slight increase in MMP was also observed when the algae were treated with f-MWCNT alone. The buildup of intracellular ROS may lead to a rise in MMP, which would then impair the functioning of the mitochondria (Amado and Monserrat 2010). Mikhailov et al. (2003) found that nanoparticles may attach to the beta subunit of ATP synthase, which can amplify mitochondrial membrane depolarization, disrupt the electron transport chain, and generate reactive oxygen species. A recent study by Wang et al. (2021) noted an increase in the mitochondrial membrane potential of the freshwater algae *Chlorella pyrenoidosa* when exposed to graphene oxide (GO) alone and combined with nano-zirconium oxide.

The esterase activity was significantly reduced when the algae were exposed to graphene, f-MWCNT, and graphene-f-MWCNT mixture. This can be related to the disruption of the cells by oxidative stress and a decrease in cell metabolism activity (Melegari et al. 2013). Martín-de-Lucía et al. (2018) observed decreased esterase activity and increased oxygen species of algae *Chlamydomonas reinhardtii* when treated with graphene oxide and graphene oxide-wastewater combined. Cruces et al. (2021) exposed the algal cells *Microcystis aeruginosa* to graphene oxide and graphene oxide-oxidized multi-walled carbon nanotube mixture. They observed increased oxidative stress and a decrease in photosynthetic and esterase activities. They also noted that a reduction of esterase activity could be attributed to oxidative stress, cell structure damage, or damage to the photosynthetic centers.

Conclusion

In this study, we investigated the toxic effects of graphene, f-MWCNT, and the combination of these two carbon nanomaterials in a freshwater alga. We note that graphene and the binary mixture generated cellular oxidative stress, activated antioxidant defense systems, and disrupted photosynthetic activity in *S. obliquus*, whereas f-MWCNT did not cause severe stress. Increased radical generation led to membrane disruptions and reduced the photosynthetic efficiency and the flow of electrons, interfering with the cell's ability to function normally. The results also emphasize that the binary combination of graphene and f-MWCNT caused increased damage to the algal cells than the individual nanomaterials. To better comprehend the ecological risks of various CNMs, future studies should include combinations of multiple CNMs and CNMs with other inorganic and organic

pollutants. The effects of natural organic materials in the aquatic environment on the toxic effects also need to be examined to extrapolate the outcomes to real environmental situations. Future toxicity studies should also account for additional environmental parameters such as pH, water flow velocity, and different nanoparticle concentrations.

Supplementary Information The online version contains supplementary material available at <https://doi.org/10.1007/s11356-023-27367-6>.

Acknowledgements The authors thank the Centre for Fire, Explosives, and Environment Safety, Timarpur, Delhi 110054, India, and the Vellore Institute of Technology (VIT) for providing the nanomaterials and SEM facilities used in this study.

Author contribution **Soupan Das**: investigation, methodology, visualization, formal analysis, writing—review and editing. **Sayani Giri**: writing—original draft. **Gaurav Wadhwa**: investigation and methodology. **Mrudula Pulimi**: conceptualization, methodology, supervision, writing—review and editing. **Shalini Anand**: conceptualization, methodology, supervision, writing—review and editing. **Natarajan Chandrasekaran**: formal analysis, resources. **Seyed Ali Johari**: formal analysis, writing—review and editing. **Pramod Kumar Rai**: conceptualization, methodology, supervision, writing—review and editing. **Amitava Mukherjee**: conceptualization, methodology, supervision, project administration, writing—review and editing.

Funding The study was carried out using the funds provided by CFEES-DRDO (Sanction No. CFEES/TCP/EnSG/CARS(P)/DG(SAM)/FTS-ERAF/VIT-VELLORE). The authors would also like to thank Sh. Rajiv Narang (Outstanding Scientist and Director), Centre for Fire, Explosives, and Environment Safety-Defence Research and Development Organisation (CFEES-DRDO) for funding this research.

Data availability All data employed in support of the outcomes of the study are included in the article.

Declarations

Ethical approval Not applicable.

Consent to participate It is declared that the study involved no human participants.

Consent for publication All authors have given consent to the publication of the manuscript.

Competing interests The authors declare no competing interests.

References

- Amado LL, Monserrat JM (2010) Oxidative stress generation by microcystins in aquatic animals: why and how. *Environ Int* 36:226–235
- Arvidsson R, Molander S, Sandén BA (2013) Review of potential environmental and health risks of the nanomaterial graphene. *Hum Ecol Risk Assess Int J* 19:873–887
- Barbieri E, Campos-Garcia J, Martinez DS, da Silva JRM, Alves OL, Rezende KF (2016) Histopathological effects on gills of Nile Tilapia (*Oreochromis niloticus*, Linnaeus, 1758) exposed to Pb and carbon nanotubes. *Microsc Microanal* 22:1162–1169
- Begum P, Fugetsu B (2013) Induction of cell death by graphene in *Arabidopsis thaliana* (Columbia ecotype) T87 cell suspensions. *J Hazard Mater* 260:1032–1041
- Borza C, Muntean D, Dehelean C, Săvoiu G, Șerban C, Simu G, Andoni M, Butur M, Drăgan S, (2013) Oxidative stress and lipid peroxidation—a lipid metabolism dysfunction. *Lipid Metab* 34:23–38
- Bundschuh M, Filser J, Lüderwald S, McKee MS, Metreveli G, Schaumann GE, Schulz R, Wagner S (2018) Nanoparticles in the environment: where do we come from, where do we go to? *Environ Sci Eur* 30:1–17
- Chakraborty D, Ethiraj K, Chandrasekaran N, Mukherjee A (2021) Mitigating the toxic effects of CdSe quantum dots towards freshwater alga *Scenedesmus obliquus*: role of eco-corona. *Environ Pollut* 270:116049
- Christian P, Von der Kammer F, Baalousha M, Hofmann T (2008) Nanoparticles: structure, properties, preparation and behaviour in environmental media. *Ecotoxicology* 17:326–343
- Cruces E, Barrios AC, Cahue YP, Januszewski B, Gilbertson LM, Perreault F (2021) Similar toxicity mechanisms between graphene oxide and oxidized multi-walled carbon nanotubes in *Microcystis aeruginosa*. *Chemosphere* 265:129137
- Dallavalle M, Calvaresi M, Bottoni A, Melle-Franco M, Zerbetto F (2015) Graphene can wreak havoc with cell membranes. *ACS Appl Mater Interfaces* 7:4406–4414
- Fang R, Gong J, Cao W, Chen Z, Huang D, Ye J, Cai Z (2022) The combined toxicity and mechanism of multi-walled carbon nanotubes and nano copper oxide toward freshwater algae: *Tetradasmus obliquus*. *J Environ Sci* 112:376–387
- Finaud J, Lac G, Filaire E (2006) Oxidative stress. *Sports Medicine* 36:327–358
- Freixa A, Acuña V, Sanchís J, Farré M, Barceló D, Sabater S (2018) Ecotoxicological effects of carbon based nanomaterials in aquatic organisms. *Sci Total Environ* 619:328–337
- Guo C, Song P, Cao X (2016) Effect of citric acid on toxicity of graphene towards freshwater algae (*Chlorella pyrenoidosa*), 2016 5th International Conference on Environment, Materials, Chemistry and Power Electronics. Atlantis Press
- Guo X, Mei N (2014) Assessment of the toxic potential of graphene family nanomaterials. *J Food Drug Anal* 22:105–115
- Guo Y-Y, Zhang J, Zheng Y-F, Yang J, Zhu X-Q (2011) Cytotoxic and genotoxic effects of multi-wall carbon nanotubes on human umbilical vein endothelial cells in vitro. *Mutat Res/Genet Toxicol Environ Mutagen* 721:184–191
- Hazeem LJ, Bououdina M, Dewailly E, Slomianny C, Barras A, Coffinier Y, Szunerits S, Boukherroub R (2017) Toxicity effect of graphene oxide on growth and photosynthetic pigment of the marine alga *Picochlorum* sp. during different growth stages. *Environ Sci Pollut Res* 24:4144–4152
- Hu C, Wang Q, Zhao H, Wang L, Guo S, Li X (2015a) Ecotoxicological effects of graphene oxide on the protozoan *Euglena gracilis*. *Chemosphere* 128:184–190
- Hu L, Chen J, Wei Y, Wang M, Xu Y, Wang C, Gao P, Liu Y, Liu C, Song Y (2023) Photocatalytic degradation effect and mechanism of *Karenia mikimotoi* by non-noble metal modified TiO₂ loading onto copper metal organic framework (SNP-TiO₂@ Cu-MOF) under visible light. *J Hazard Mater* 442:130059
- Hu X, Ouyang S, Mu L, An J, Zhou Q (2015b) Effects of graphene oxide and oxidized carbon nanotubes on the cellular division, microstructure, uptake, oxidative stress, and metabolic profiles. *Environ Sci Technol* 49:10825–10833
- Iswarya V, Bhuvaneshwari M, Alex SA, Iyer S, Chaudhuri G, Chandrasekaran PT, Bhalerao GM, Chakravarty S, Raichur AM, Chandrasekaran N (2015) Combined toxicity of two crystalline phases (anatase and rutile) of Titania nanoparticles towards freshwater microalgae: *Chlorella* sp. *Aquatic toxicology* 161:154–169

- Kim KY, Kim SM, Kim JY, Choi Y-E (2022) Elucidating the mechanisms underlying the cytotoxic effects of nano-/micro-sized graphene oxide on the microalgae by comparing the physiological and morphological changes in different trophic modes. *Chemosphere* 309:136539
- Kono Y (1978) Generation of superoxide radical during autoxidation of hydroxylamine and an assay for superoxide dismutase. *Arch Biochem Biophys* 186:189–195
- Kwok KW, Leung KM, Flahaut E, Cheng J, Cheng SH (2010) Chronic toxicity of double-walled carbon nanotubes to three marine organisms: influence of different dispersion methods. *Nanomedicine* 5:951–961
- Li W, Liang C, Zhou W, Qiu J, Zhou Z, Sun G, Xin Q (2003) Preparation and characterization of multi-walled carbon nanotube-supported platinum for cathode catalysts of direct methanol fuel cells. *J Phys Chem B* 107:6292–6299
- Li X, Qiu H, Zhang P, Song L, Romero-Freire A, He E (2023) Role of heteroaggregation and internalization in the toxicity of differently sized and charged plastic nanoparticles to freshwater microalgae. *Environ Pollut* 316:120517
- Lin M-Y (2008) Interactions between titanium dioxide nanoparticles and algal cells at moderate particle concentration. University of Delaware, Newark, p 1457124
- Liu W, Au DW, Anderson DM, Lam PK, Wu RS (2007) Effects of nutrients, salinity, pH and light: dark cycle on the production of reactive oxygen species in the alga *Chattonella marina*. *J Exp Mar Biol Ecol* 346:76–86
- Liu X, Wang X, Zhang F, Yao X, Qiao Z, Deng J, Jiao Q, Gong L, Jiang X (2022) Toxic effects of fludioxonil on the growth, photosynthetic activity, oxidative stress, cell morphology, apoptosis, and metabolism of *Chlorella vulgaris*. *Sci Total Environ* 838:156069
- Long Z, Ji J, Yang K, Lin D, Wu F (2012) Systematic and quantitative investigation of the mechanism of carbon nanotubes' toxicity toward algae. *Environ Sci Technol* 46:8458–8466
- Lukhele LP, Mamba BB, Musee N, Wepener V (2015) Acute toxicity of double-walled carbon nanotubes to three aquatic organisms. *J Nanomater* 2015:3–3
- Lv B, Wang C, Hou J, Wang P, Miao L, Li Y, Ao Y, Yang Y, You G, Xu Y (2016) Influence of shear forces on the aggregation and sedimentation behavior of cerium dioxide (CeO₂) nanoparticles under different hydrochemical conditions. *J Nanopart Res* 18:1–12
- Machado MD, Soares EV (2015) Use of a fluorescence-based approach to assess short-term responses of the alga *Pseudokirchneriella subcapitata* to metal stress. *J Appl Phycol* 27:805–813
- Malhotra N, Villaflores OB, Audira G, Siregar P, Lee J-S, Ger T-R, Hsiao C-D (2020) Toxicity studies on graphene-based nanomaterials in aquatic organisms: Current understanding. *Molecules* 25:3618
- Manna SK, Sarkar S, Barr J, Wise K, Barrera EV, Jejelowo O, Rice-Ficht AC, Ramesh GT (2005) Single-walled carbon nanotube induces oxidative stress and activates nuclear transcription factor- κ B in human keratinocytes. *Nano Lett* 5:1676–1684
- Markus AA, Parsons JR, Roex EW, Voogt Pd, Laane RW (2016) Modelling the release, transport and fate of engineered nanoparticles in the aquatic environment—a review. *Rev Environ Contam Toxicol* 243:53–87
- Martín-de-Lucía I, Campos-Mañas MC, Agüera A, Leganés F, Fernández-Piñas F, Rosal R (2018) Combined toxicity of graphene oxide and wastewater to the green alga *Chlamydomonas reinhardtii*. *Environ Sci Nano* 5:1729–1744
- Martinez D, Alves O, Barbieri E (2013) Carbon nanotubes enhanced the lead toxicity on the freshwater fish. *J Phys Conf Ser* 429:012043. IOP Publishing, Bristol
- Melegari SP, Perreault F, Costa RHR, Popovic R, Matias WG (2013) Evaluation of toxicity and oxidative stress induced by copper oxide nanoparticles in the green alga *Chlamydomonas reinhardtii*. *Aquat Toxicol* 142:431–440
- Mikhailov A, Härmälä-Braskén A-S, Hellman J, Meriluoto J, Eriksson JE (2003) Identification of ATP-synthase as a novel intracellular target for microcystin-LR. *Chem Biol Interact* 142:223–237
- Natarajan L, Omer S, Jetly N, Jenifer MA, Chandrasekaran N, Suraishkumar G, Mukherjee A (2020) Eco-corona formation lessens the toxic effects of polystyrene nanoplastics towards marine microalgae *Chlorella sp.* *Environ Res* 188:109842
- Nazari F, Jafarirad S, Movafeghi A, Kosari-Nasab M, Kazemi EM (2020) Toxicity of microwave-synthesized silver-reduced graphene oxide nanocomposites to the microalga *Chlorella vulgaris*: comparison with the hydrothermal method synthesized counterparts. *J Environ Sci Health Part A* 55:639–649
- Nogueira P, Nakabayashi D, Zucolotto V (2015) The effects of graphene oxide on green algae *Raphidocelis subcapitata*. *Aquat Toxicol* 166:29–35
- OECD (2004) 202: *Daphnia sp.* acute immobilisation test. OECD Guidelines for the Testing of Chemicals, Section 2
- Owusu-Ansah E, Yavari A, Banerjee U et al (2008) A protocol for in vivo detection of reactive oxygen species. Protocol (Version 1) available at Protocol Exchange. <https://doi.org/10.1038/nprot.2008.23>
- Parks A (2013) Contaminant interactions and biological effects of single-walled carbon nanotubes in a benthic estuarine system. dukespace.lib.duke.edu
- Pikula K, Chaika V, Zakharenko A, Markina Z, Vedyagin A, Kuznetsov V, Gusev A, Park S, Golokhvast K (2020) Comparison of the level and mechanisms of toxicity of carbon nanotubes, carbon nanofibers, and silicon nanotubes in bioassay with four marine microalgae. *Nanomaterials* 10:485
- Piotrowska-Niczyporuk A, Bajguz A, Zambrzycka E, Godlewska-Zylkiewicz B (2012) Phytohormones as regulators of heavy metal biosorption and toxicity in green alga *Chlorella vulgaris* (Chlorophyceae). *Plant Physiol Biochem* 52:52–65
- Politowski, Regnery P, Hennig MP, Siebers N, Ottermanns R, Schäffer A (2021) Fate of weathered multi-walled carbon nanotubes in an aquatic sediment system. *Chemosphere* 1(277):130319
- Rezayian M, Niknam V, Ebrahimzadeh H (2019) Oxidative damage and antioxidative system in algae. *Toxicol Rep* 6:1309–1313
- Romanowska-Duda Z, Grzesik M, Janas R (2019) Maximal efficiency of PSII as a marker of sorghum development fertilized with waste from a biomass biodigestion to methane. *Front Plant Sci* 9:1920
- Roy B, Chandrasekaran H, Krishnan SP, Chandrasekaran N, Mukherjee A (2018) UVA pre-irradiation to P25 titanium dioxide nanoparticles enhanced its toxicity towards freshwater algae *Scenedesmus obliquus*. *Environ Sci Pollut Res* 25:16729–16742
- Roy B, Suresh P, Chandrasekaran N, Mukherjee A (2020) UVB pre-irradiation of titanium dioxide nanoparticles is more detrimental to freshwater algae than UVA pre-irradiation. *J Environ Chem Eng* 8:104076
- Roy B, Suresh P, Chandrasekaran N, Mukherjee A (2021) Antibiotic tetracycline enhanced the toxic potential of photo catalytically active P25 titanium dioxide nanoparticles towards freshwater algae *Scenedesmus obliquus*. *Chemosphere* 267:128923
- Rudi H, Regel JMF, Ganf GG, Brookes JD (2002) Algal esterase activity as a biomeasure of environmental degradation in a freshwater creek. *Aquat Toxicol* 59:209–223
- Saravanan N, Rajasekar R, Mahalakshmi S, Sathishkumar T, Sasi-kumar K, Sahoo S (2014) Graphene and modified graphene-based polymer nanocomposites—a review. *J Reinf Plast Compos* 33:1158–1170
- Saxena P, Sangela V, Ranjan S, Dutta V, Dasgupta N, Phulwaria M, Rathore DS (2020) Aquatic nanotoxicology: impact of carbon nanomaterials on algal flora. *Energy Ecol Environ* 5:240–252

- Schwab F, Bucheli TD, Lukhele LP, Magrez A, Nowack B, Sigg L, Knauer K (2011) Are carbon nanotube effects on green algae caused by shading and agglomeration? *Environ Sci Technol* 45:6136–6144
- Schwab F, Bucheli TD, Camenzuli L, Magrez A, Knauer K, Sigg L, Nowack B (2013) Diuron sorbed to carbon nanotubes exhibits enhanced toxicity to *Chlorella vulgaris*. *Environ Sci Technol* 47:7012–7019
- Segal M (2009) Selling graphene by the ton. *Nat Nanotechnol* 4:612–614
- Setsukinai K, Urano Y, Kakinuma K, Majima HJ, Nagano T (2003) Development of novel fluorescence probes that can reliably detect reactive oxygen species and distinguish specific species. *J Biol Chem* 278:3170–3175
- Sousa CA, Soares HM, Soares EV (2018) Toxic effects of nickel oxide (NiO) nanoparticles on the freshwater alga *Pseudokirchneriella subcapitata*. *Aquat Toxicol* 204:80–90
- Stanley JK, Laird JG, Kennedy AJ, Steevens JA (2016) Sublethal effects of multi-walled carbon nanotube exposure in the invertebrate *Daphnia magna*. *Environ Toxicol Chem* 35:200–204
- Thiagarajan V, Iswarya V, Seenivasan R, Chandrasekaran N, Mukherjee A (2019) Influence of differently functionalized polystyrene microplastics on the toxic effects of P25 TiO₂ NPs towards marine algae *Chlorella sp.* *Aquat Toxicol* 207:208–216
- Thurnherr T, Brandenberger C, Fischer K, Diener L, Manser P, Maeder-Althaus X, Kaiser J-P, Krug HF, Rothen-Rutishauser B, Wick P (2011) A comparison of acute and long-term effects of industrial multi-walled carbon nanotubes on human lung and immune cells in vitro. *Toxicol Lett* 200:176–186
- Van der Paal J, Neyts EC, Verlact CC, Bogaerts A (2016) Effect of lipid peroxidation on membrane permeability of cancer and normal cells subjected to oxidative stress. *Chem Sci* 7:489–498
- Vargas-Estrada L, Torres-Arellano S, Longoria A, Arias DM, Okoye PU, Sebastian P (2020) Role of nanoparticles on microalgal cultivation: a review. *Fuel* 280:118598
- Wang H, Jin M, Mao W, Chen C, Fu L, Li Z, Du S, Liu H (2020) Photosynthetic toxicity of non-steroidal anti-inflammatory drugs (NSAIDs) on green algae *Scenedesmus obliquus*. *Sci Total Environ* 707:136176
- Wang M, Chen J, Hu L, Wei Y, Xu Y, Wang C, Gao P, Liu Y, Liu C, Song Y (2023) Heterogeneous interfacial photocatalysis for the inactivation of *Karenia mikimotoi* by Bi₂O₃ loaded onto a copper metal organic framework (Bi₂O₃@ Cu-MOF) under visible light. *Chem Eng J* 456:141154
- Wang Z, Gao Y, Wang S, Fang H, Xu D, Zhang F (2016) Impacts of low-molecular-weight organic acids on aquatic behavior of graphene nanoplatelets and their induced algal toxicity and antioxidant capacity. *Environ Sci Pollut Res* 23:10938–10945
- Wang Z, Zhang F, Vijver MG, Peijnenburg WJ (2021) Graphene nanoplatelets and reduced graphene oxide elevate the microalgal cytotoxicity of nano-zirconium oxide. *Chemosphere* 276:130015
- Wei L, Thakkar M, Chen Y, Ntım SA, Mitra S, Zhang X (2010) Cytotoxicity effects of water dispersible oxidized multi-walled carbon nanotubes on marine alga, *Dunaliella tertiolecta*. *Aquat Toxicol* 100:194–201
- Yin J, Dong Z, Liu Y, Wang H, Li A, Zhuo Z, Feng W, Fan W (2020a) Toxicity of reduced graphene oxide modified by metals in microalgae: effect of the surface properties of algal cells and nanomaterials. *Carbon* 169:182–192
- Yin J, Fan W, Du J, Feng W, Dong Z, Liu Y, Zhou T (2020b) The toxicity of graphene oxide affected by algal physiological characteristics: a comparative study in cyanobacterial, green algae, diatom. *Environ Pollut* 260:113847
- Zhang L, Lei C, Chen J, Yang K, Zhu L, Lin D (2015) Effect of natural and synthetic surface coatings on the toxicity of multi-walled carbon nanotubes toward green algae. *Carbon* 83:198–207
- Zhang L, Li J, Yang K, Liu J, Lin D (2016) Physicochemical transformation and algal toxicity of engineered nanoparticles in surface water samples. *Environ Pollut* 211:132–140
- Zhang Y, Meng T, Shi L, Guo X, Si X, Yang R, Quan X (2019) The effects of humic acid on the toxicity of graphene oxide to *Scenedesmus obliquus* and *Daphnia magna*. *Sci Total Environ* 649:163–171
- Zhao J, Wang Z, White JC, Xing B (2014) Graphene in the aquatic environment: adsorption, dispersion, toxicity and transformation. *Environ Sci Technol* 48:9995–10009
- Zhao J, Cao X, Wang Z, Dai Y, Xing B (2017) Mechanistic understanding toward the toxicity of graphene-family materials to freshwater algae. *Water Res* 111:18–27
- Zhao J, Lin M, Wang Z, Cao X, Xing B (2021) Engineered nanomaterials in the environment: are they safe? *Crit Rev Environ Sci Technol* 51(14):1443–1478
- Zhou D, Bennett SW, Keller AA (2012) Increased mobility of metal oxide nanoparticles due to photo and thermal induced disagglomeration. *PLoS ONE* 7:e37363
- Zhu S, Zhu B, Huang A, Hu Y, Wang G, Ling F (2016) Toxicological effects of multi-walled carbon nanotubes on *Saccharomyces cerevisiae*: the uptake kinetics and mechanisms and the toxic responses. *J Hazard Mater* 318:650–662
- Zhu X, Tan L, Zhao T, Huang W, Guo X, Wang J, Wang J (2022) Alone and combined toxicity of ZnO nanoparticles and graphene quantum dots on microalgae *Gymnodinium*. *Environ Sci Pollut Res* 29(31):47310–47322. <https://doi.org/10.1007/s11356-022-19267-y>
- Zindler F, Glomstad B, Altin D, Liu J, Jenssen BM, Booth AM (2016) Phenanthrene bioavailability and toxicity to *Daphnia magna* in the presence of carbon nanotubes with different physicochemical properties. *Environ Sci Technol* 50:12446–12454

Publisher's note Springer Nature remains neutral with regard to jurisdictional claims in published maps and institutional affiliations.

Springer Nature or its licensor (e.g. a society or other partner) holds exclusive rights to this article under a publishing agreement with the author(s) or other rightsholder(s); author self-archiving of the accepted manuscript version of this article is solely governed by the terms of such publishing agreement and applicable law.